Laboratory testing of Beerkan infiltration experiments for assessing the role of soil sealing on water infiltration

Laboratory testing of Beerkan infiltration experiments for assessing the role of soil sealing on water infiltration

Article *in* Catena · August 2018

DOI: 10.1016/j.catena.2018.05.013

CITATIONS
33

READS
1,120

7 authors, including:

Simone Di Prima
Università degli Studi di Sassari
96 PUBLICATIONS **1,059** CITATIONS
SEE PROFILE

Paola Concialdi
Università degli Studi di Palermo
10 PUBLICATIONS **42** CITATIONS
SEE PROFILE

Laurent Lassabatere
Ecole Nationale des Travaux Publics de l'Etat
189 PUBLICATIONS **1,804** CITATIONS
SEE PROFILE

Mario Pirastru
Università degli Studi di Sassari
44 PUBLICATIONS **407** CITATIONS
SEE PROFILE

Laboratory testing of Beerkan infiltration experiments for assessing the role of soil sealing on water infiltration

S. Di Prima[1,*], P. Concialdi[2], L. Lassabatere[3], R. Angulo-Jaramillo[3], M. Pirastru[1], A. Cerdà[4], S.Keesstra[5]

[1] Agricultural Department, University of Sassari, Viale Italia, 39, 07100 Sassari, Italy
[2] Department of Agricultural, Food and Forest Sciences, University of Palermo, Viale delle Scienze, 90128 Palermo, Italy
[3] Université de Lyon; UMR5023 Ecologie des Hydrosystèmes Naturels et Anthropisés; CNRS ; ENTPE ; Université Lyon 1; 3 rue Maurice Audin, 69518 Vaulx-en-Velin, France
[4] Department of Geography, University of Valencia, Blasco Ibáñez, 28, 46010 València, Spain
[5] Team Soil Water and Land Use, Wageningen Environmental Research, Wageningen UR, Droevendaalsesteeg 3, 6700 AA Wageningen, The Netherlands
* Corresponding Author. E-mail: sdiprima@uniss.it

This is a post-refereeing final draft. When citing, please refer to the published version:

Di Prima, S., Concialdi, P., Lassabatere, L., Angulo-Jaramillo, R., Pirastru, M., Cerda, A., Keesstra, S., 2018. Laboratory testing of Beerkan infiltration experiments for assessing the role of soil sealing on water infiltration. CATENA 167, 373–384. https://doi.org/10.1016/j.catena.2018.05.013

Abstract

Soil surface sealing is a major cause of decreased infiltration rates and increased surface runoff and erosion during a rainstorm. The objective of this paper is to quantify the effect of surface sealing on infiltration for 3 layered soils with different textures for the upper layer and investigate the capability of BEST procedure to catch the formation of the seal and related consequences on water infiltration. Rainfall experiments were carried out to induce the formation of the seal. Meanwhile, Beerkan infiltration runs were carried out pouring water at different distances from the soil surface (BEST-H versus BEST-L runs, with a High and Low water pouring heights, respectively) for the same type of layered soils. Then, we determined saturated soil hydraulic conductivity, K_s, values from rainfall simulation and Beerkan infiltration experiments. Rainfall simulations carried out on soil layers having different depths allowed to demonstrate that infiltration processes were mainly driven by the seal and that K_s estimates were representative of the seal. Mean K_s values, estimated for the late-phase, ranged from 13.9 to 26.2 mm h^{-1}. Soil sealing induced an increase in soil bulk density by 38.7 to 42.1%, depending on the type of soil. Rainfall-deduced K_s data were used as target values and compared with those estimated by the Beerkan runs. BEST-H runs proved more appropriate than BEST-L runs, those last triggering no seal formation. The predictive potential of the three BEST algorithms (BEST-slope, BEST-intercept and BEST-steady) to yield a proper K_s estimate for the seal was also investigated. BEST-slope yielded negative K_s values in 87% of the cases for BEST-H runs. Positive values were obtained in 100% of the cases with BEST-steady and BEST-intercept. However, poorer fits were obtained with the latter algorithm. The comparison of K_s estimates with rainfall-deduced estimates allowed to identify BEST-steady algorithm with BEST-H run as the best combination. The method proposed in this study could be used to easily measure the seal's saturated hydraulic conductivity of an initially undisturbed bare soil directly impacted by water with minimal experimental efforts, using small volumes of water and easily transportable equipment.

Keywords: Soil sealing, Rainfall simulation, Beerkan infiltration experiment, BEST algorithms, Saturated soil hydraulic conductivity.

1. Introduction

Droplet impact during a rainfall event can modify surface soil structure and determines the splash erosion (e.g., Assouline and Mualem, 2002; Fernández-Raga et al., 2017). The compaction of fine material from the disrupted and dispersed aggregates may form a thin and highly dense layer (Mualem and Assouline, 1989). This surface sealing is a major cause of decreased infiltration rates and increased surface runoff and erosion during a rainstorm (Moldenhauer and Long, 1964). The formation of seals is dominated by a wide variety of factors involving soil properties, rainfall characteristics, and flow conditions (Assouline, 2004). The determination of seal hydraulic properties, as well as their evolution over time, is one of the key issues in properly describing water flow in soils (Augeard et al., 2007).

There are two main methodological approaches to measure the infiltration of the soil: rainfall simulations and water infiltration techniques using either ring or tension disk infiltrometers (Angulo-Jaramillo et al., 2016). Among the water infiltration techniques, the Beerkan method consists in infiltrating water through a ring under ponded conditions (Braud et al., 2005). Lassabatere et al. (2006) developed the BEST algorithm (Beerkan estimation of Soil pedoTransfer functions) to derive the whole set of soil hydraulic parameters related to water retention and unsaturated hydraulic conductivity curves from Beerkan experimental data. Ever

Di Prima, S., Concialdi, P., Lassabatere, L., Angulo-Jaramillo, R., Pirastru, M., Cerda, A., Keesstra, S., 2018. Laboratory testing of Beerkan infiltration experiments for assessing the role of soil sealing on water infiltration. CATENA 167, 373–384. https://doi.org/10.1016/j.catena.2018.05.013

since, three main algorithms were developed on the basis of this first version: BEST-slope (Lassabatere et al., 2006), BEST-intercept (Yilmaz et al., 2010) and BEST-steady (Bagarello et al., 2014a). The three algorithms make use of the same input data, but differ from the way they fit experimental data to the models for transient and steady states (Angulo-Jaramillo et al., 2016; Lassabatere et al., 2013). These differences allow one of the three methods to perform better according to the kind of soil. Beerkan runs and BEST calculations, also referred to as BEST procedure, are spread worldwide for the characterization of the hydraulic properties of uniform soils (Angulo-Jaramillo et al., 2016).

To study seal formation, most research studies in the last decades were performed with rainfall simulations, either during its dynamic stage or after it has already reached its final stage, when the seal layer is fully developed (e.g., Assouline, 2004; Baumhardt et al., 1990). Rainfall experiments are an attractive tool because the precision, accuracy and the possibility of high repetition rate offer a systematic approach to address the different factors that influence the studied processes (Iserloh et al., 2013). Besides, the use of water infiltration techniques for assessing soil sealing impacts on water infiltration is still largely unknown notwithstanding that these methods have a noticeable practical interest (Bagarello et al., 2014b). Moreover, the use of ring or tension disk infiltrometers still presents a number of problems related both to theory and practice for data collected on heterogeneous layered soils (Angulo-Jaramillo et al., 2000); which is the case of sealed soils. Under such conditions, the steady-state water flow analysis based on usual analysis procedures are generally found to be inadequate (Logsdon and Jaynes, 1993). Besides, infiltrometer data are generally analyzed by assuming that the sampled porous medium is rigid, homogeneous, isotropic and uniformly unsaturated before the run (Alagna et al., 2013, e.g., 2017, Lassabatere et al., 2006, 2009; Reynolds and Elrick, 1990). However, when soil sealing occurs, the soil shifts from uniform to finely layered state. Lastly, the regular Beerkan runs that apply water at soil surface do not trigger any soil sealing; which fails to represent the real soil hydraulic behavior during intense rainfall events.

Recently, Di Prima et al. (2017) adapted the BEST infiltration procedure to mimic rainfall simulation experiments. These authors adapted the height of application of water (still maintaining ponding at surface) for mimicking the impacts of raindrops on soil surface. They demonstrated that both rainfall simulation experiments and modified Beerkan runs, carried out by applying water at a relatively large distance from the soil surface (BEST-H procedure), determine a similar degree of soil compaction and mechanical breakdown of aggregates, but the second ones are much easier to conduct. Moreover, the BEST-H procedure is easy to apply over large areas since the equipment to be transported is minimal and small volumes of water are enough to conduct an infiltration run. BEST-H runs can simply be replicated to develop a large number of sampling points, which means that intensive sampling over a large or relatively large areas is feasible (Gonzalez-Sosa et al., 2010). BEST procedures also allow to survey remote areas, which are difficult for other methods with heavy, expensive, time spending procedures and labor high costs (Bagarello et al., 2011). However, the comparison of BEST-H procedure with well tested methods for K_s estimation, such as rainfall simulation experiments, is necessary to experimentally assess the predictive performances of BEST for the case of soil sealing. Indeed, in the scientific literature there is no exhaustive testing of the relative performances of the BEST algorithms with regards to the specific case of layered and sealed soils.

The objectives of this research were to: (i) measure the effect of surface sealing on infiltration at the surface of three bare soils with different textures exposed to the direct impact of raindrops, (ii) evaluate the influence of the thickness of the upper layer of soil on seal formation and related impacts on water infiltration, (iii) compare ponded infiltrometer runs (Beerkan runs) with rainfall simulation experiments in terms of saturated soil hydraulic conductivity for the case of soil sealing, and (iv) investigate which BEST algorithm can be satisfactorily adopted to properly estimate K_s of the seal.

2. Material and methods

2.1. Soil sampling

Soil materials used in this study were taken from Ap horizons of three Sicilian sites with different physical properties (Bagarello et al., 2014a). According to the USDA classification, a sandy-loam (SL) soil and a clay-loam (CL) soil were sampled at the Department of Agriculture, Food and Forest Sciences of the Palermo University. A clay (C) soil was sampled at the experimental station for soil erosion measurement at Sparacia (University of Palermo), approximately 100 km south of Palermo. Particle size distribution (PSD) was determined following H_2O_2 pre-treatment to eliminate organic matter and clay deflocculation using sodium hexametaphosphate and mechanical agitation (Gee and Bauder, 1986). In particular, fine size fractions were determined by the hydrometer method, whereas the coarse fractions were obtained by mechanical dry sieving. The soil organic carbon content, OC (%), was determined by the Walkley–Black method (Nelson and Sommers, 1996). Then, the soil organic matter content, OM (%), was estimated using the van Bemmelen conversion factor of 1.724 (Van Bemmelen, 1890). Each soil was air-dried, ground to an aggregate or particle diameter slightly larger than 2 mm, and sieved through a 2-mm mesh (Bradford et al., 1987). The measured soil physical properties are summarized in **Table 1**.

2.2. Rainfall simulation experiments

Many laboratory as well as field studies have been conducted over more than five decades on the formation of seals at the surface of bare soils exposed to the direct impact of

Di Prima, S., Concialdi, P., Lassabatere, L., Angulo-Jaramillo, R., Pirastru, M., Cerda, A., Keesstra, S., 2018. Laboratory testing of Beerkan infiltration experiments for assessing the role of soil sealing on water infiltration. CATENA 167, 373–384. https://doi.org/10.1016/j.catena.2018.05.013

Table 1. Coordinates, soil textural classification, clay (0–2 μm), silt (2–50 μm), and sand (50–2000 μm) content (in %) (USDA classification system) in the 0-10 cm depth range, soil organic matter (OM in %) content, dry soil bulk density (ρ_b in g cm^{-3}), and initial volumetric soil water content (θ_0 in cm^3cm^{-3}), for the three sampled soils. Standard deviations are indicated in parentheses.

Coordinates	33S 355511 E 4218990 N	33S 355341 E 4219012 N	33S 391172 E 4166165 N
Textural classification	Sandy-loam	Clay-loam	Clay
Clay	17.6 (1.9)	29.9(2.8)	71.5 (1.8)
Silt	29.8 (2.8)	34.1(1.8)	23.6 (1.4)
Sand	52.6 (4.7)	36.0(1.2)	4.9 (0.8)
OM	3.9(0.7)	2.3(0.1)	1.1(0.6)
ρ_b	0.936 (0.008)	0.984 (0.018)	1.065 (0.029)
θ_0	0.062 (0.001)	0.039 (0.001)	0.059 (0.002)

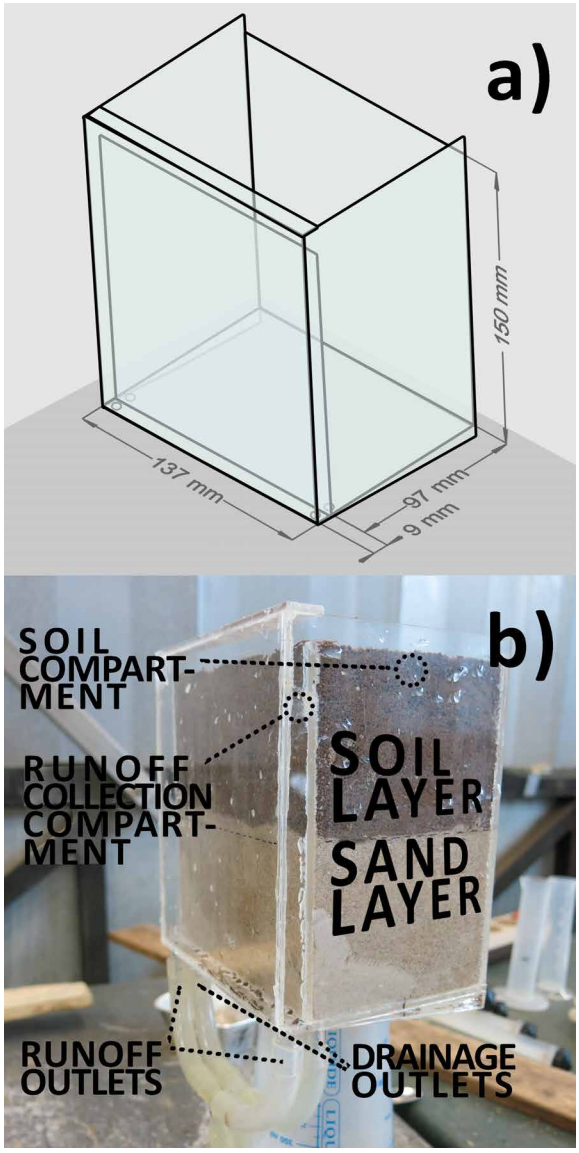

Figure 1. **(a)** Schematic diagram and **(b)** set-up of the rainfall box.

raindrops (e.g., Bradford et al., 1987; Lado et al., 2004; Tackett and Pearson, 1965; Touma et al., 2011). Laboratory experiments carried out on packed samples have the clear advantage to overcome the effects of soil heterogeneities and spatial variability on K_s measurements (Liu et al., 2011). In this investigation, we used the rainfall simulator of the Kraijenhoff van de Leur Laboratory for Water and Sediment Dynamics at Wageningen University, the Netherlands. A detailed description of the rainfall simulator is given in Lassu et al. (2015). A Lechler nozzle (nr. 460.788) was used to apply water from a 3.85-m height. In this study, a total of thirty storms were simulated at rainfall intensity R = 60 mm h^{-1}. The experiments were carried out on small rectangular soil plots encased in a transparent plexiglass box. The box set-up had two compartments: a soil compartment (1.3×10^{-2} m^2 plot area), and a runoff collection compartment, which was covered to prevent direct access of rainfall (**Figure 1**). This compartment was aimed at receiving runoff water over the soil. Each compartment had its own outlet to measure water runoff at surface and infiltration through the whole soil profile.

Following the procedure suggested by Bradford et al. (1987), the soil was compacted into the rainfall box and initial bulk density, determined from mass of soil and air-dried moisture content (**Table 1**). Soil material was added until the soil was levelled with the top of the box.

Then, the box was placed at a 9% slope under the laboratory simulator. Surface runoff from the runoff collection compartment was collected at 3 min intervals from the moment at which the runoff started to run out of the outlets until the differences in the measured runoff rates became negligible, signaling a steady-state process. The steady-state runoff rates, r (mm h^{-1}), were estimated considering the runoff rates of the last stage of the experiments, describing the steady-state phase of the process. Then, the infiltration curves were drawn by subtracting the runoff rates from the rainfall intensity (Di Prima et al., 2017). At steady state, when the soil surface is submitted to water ponding, the 1D vertical infiltration rate approaches the saturated soil hydraulic conductivity (Reynolds et al., 2000). Therefore, K_s was estimated from the rainfall simulation experiments as follows (White et al., 1989):

$$K_s = R - r \quad (1)$$

where R and r stand respectively for imposed rainfall rate and runoff rate. After each rainfall run the thickness of the seal layer was measured using a ruler.

Two different thicknesses of the soil layer were considered in this investigation. In particular, fifteen rainfall simulations (RS experiments), five for each soil, were carried out placing a 75-mm layer of soil over a 75-mm layer of sand in the soil compartment of the rainfall box (**Figure 1b**). After visually evaluating the thickness of the seals formed during the RS experiments (**Figure 2**), we settled up another fifteen rainfall simulations placing a thin (RS-T experiments) layer of soil (~1-2 mm deep) over a ~148-149 mm layer of sand. Those latter experiments were designed in order to obtain, at the end of the simulation, a fully developed seal made of the studied soil

Di Prima, S., Concialdi, P., Lassabatere, L., Angulo-Jaramillo, R., Pirastru, M., Cerda, A., Keesstra, S., 2018. Laboratory testing of Beerkan infiltration experiments for assessing the role of soil sealing on water infiltration. CATENA 167, 373–384. https://doi.org/10.1016/j.catena.2018.05.013

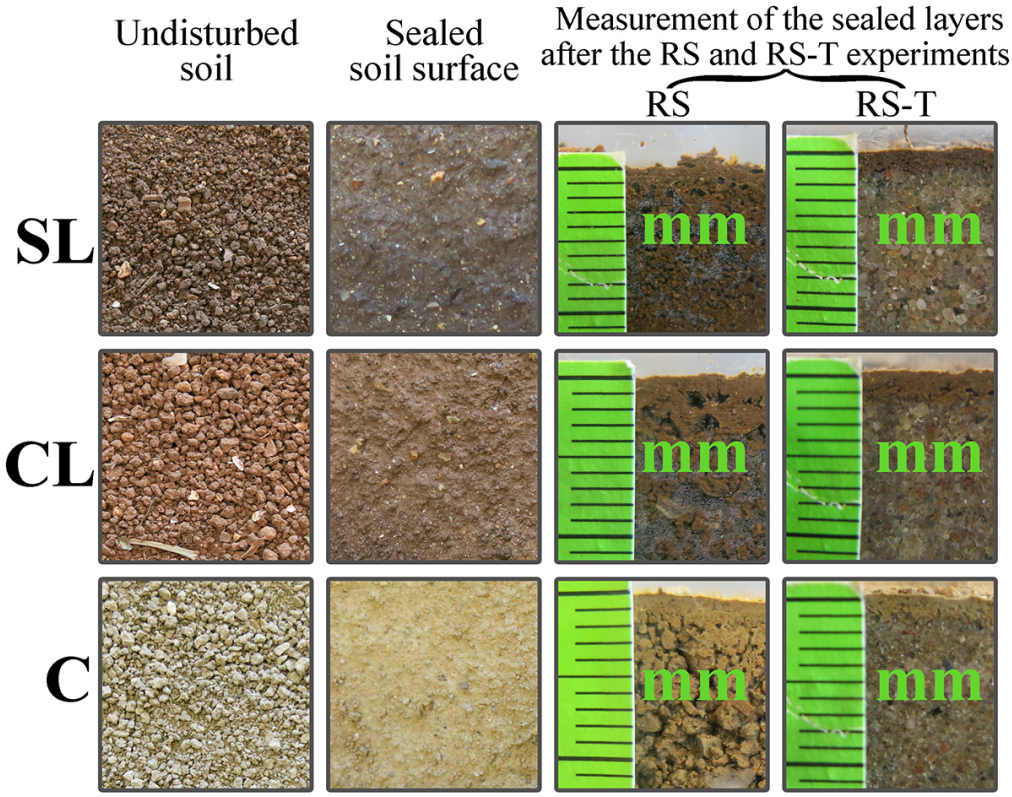

Figure 2. Pictures of the undisturbed and sealed soil surfaces before and after the rainfall simulation experiments and measurement of the sealed layers after the rainfall simulation experiments carried out on thick (RS) and thin (RS-T) soil layer for the three soils (sandy-loam, SL, clay-loam, CL, and clay, C).

above the sand (**Figure 2**). For this system, we consider that the contrast in hydraulic conductivity between the seal and the sand below is so high that the efficient hydraulic conductivity of the layered system approaches that of the seal alone, as already suggested for stratified media (e.g., Lassabatere et al., 2010; Slimene et al., 2017). In other words, the system seal above sand mimic perfectly the behavior of the seal alone.

This strategy has two advantages. Firstly, this strategy allowed the easily sampling of the seal for bulk density measurement. Before sampling, we visually verified that the seals formed over each studied soil and the sand were comparable and thus with similar physical and hydraulic properties. A sample of the seal layer was collected after each RS-T run using a 50-mm diameter ring. The risk of compaction or shattering of the sampled soil volume was minimized since the thin seal layer could be easily separated from the underlining sand layer, in opposite to the case of RS experiments. These samples were used to determine the dry bulk density of the seal layer. Moreover, this strategy was adopted in order to evaluate the influence of the seal at the late-phase of the infiltration process. In addition, we may expect that for any layered system, the efficient hydraulic properties may approach that of the seal, as soon as the seal is entirely formed and exhibits a much lower saturated hydraulic conductivity. In such case, final infiltration rates for both RS and RS-T experiments should be similar. The comparison of their values between RS and RS-T experiments allows the assessment of such hypothesis.

2.3. Concept of the BEST algorithms

BEST algorithms consider soil hydraulic properties follow van Genuchten model (1980) with Burdine (1953) condition for water retention curve and Brooks and Corey (1964) capillary function for hydraulic conductivity curve:

$$\frac{\theta-\theta_r}{\theta_s-\theta_r}=\left[1+\left(\frac{h}{h_g}\right)^n\right]^{-m} \quad (2a)$$

$$m=1-\frac{1}{n} \quad (2b)$$

$$\frac{K(\theta)}{K_s}=\left(\frac{\theta-\theta_r}{\theta_s-\theta_r}\right)^{\eta} \quad (3a)$$

$$\eta=\frac{2}{m\times n}+2+p \quad (3b)$$

where θ ($cm^3\ cm^{-3}$) is the volumetric soil water content, θ_r and θ_s are residual and saturated water contents, h (mm) is the water pressure head, h_g (mm) is the scale parameter for water pressure head, K ($mm\ h^{-1}$) is the soil hydraulic conductivity, K_s

Di Prima, S., Concialdi, P., Lassabatere, L., Angulo-Jaramillo, R., Pirastru, M., Cerda, A., Keesstra, S., 2018. Laboratory testing of Beerkan infiltration experiments for assessing the role of soil sealing on water infiltration. CATENA 167, 373–384. https://doi.org/10.1016/j.catena.2018.05.013

(mm h^{-1}) is the saturated hydraulic conductivity, *n*, *m* and η are shape parameters, and *p* is a tortuosity parameter taken equal to unity in agreement with Burdine condition (Lassabatere et al., 2006). BEST considers that residual water content is negligible, leading to $\theta_r \approx 0$. The three different BEST algorithms estimate the shape parameters *n*, *m* and η from the particle size distribution, using the same pedotransfer functions described in Lassabatere et al. (2006). And conversely, they differ from the way to estimate scale parameters h_g and K_s from cumulative infiltration data (See Appendix A). However, all the algorithms rely on the same mathematical framework for modelling Beerkan runs.

2.4. Beerkan infiltration runs and different heights of water pouring

A total of 30 Beerkan infiltration experiments were carried out, ten for each sampled soil, in laboratory plexiglass cylinders (200 mm diameter and 300 mm high). The cylinders were packed with the soil material following the same procedure adopted to fill the rainfall box. According to Bagarello et al. (2014a), a relatively small diameter of the ring (i.e., 50 mm) was chosen to detect more clearly the potential effects of soil disturbance due to water. Rings were gently inserted to a depth of 10 mm to prevent soil compaction and water leaking at surface. Following the BEST procedure suggested by Lassabatere et al. (2006), a known volume of water (17 mL) was poured in the ring at the start of the measurement and the elapsed time during the infiltration was measured. When the amount of water had completely infiltrated, an identical amount of water was poured into the ring, and the time needed for the water to infiltrate was logged. The procedure was repeated until the difference in infiltration time of the poured water volumes became negligible, signaling a practically steady-state infiltration. For each studied soil, five runs were carried out by pouring water at a small height above soil surface, i.e. at a height of 30 mm (Low, BEST-L runs). The energy was dissipated with the fingers, in an attempt to minimize soil disturbance due to water application, as commonly suggested (Reynolds, 1993). Water was applied from 250 mm height for the other 5 runs (High, BEST-H runs). In this case, the soil surface was not shielded to maximize possible damaging effects of water impact. For each infiltration run, cumulative infiltration, *I* (mm), was plotted against time, *t* (s), and a linear regression line was fitted to the last data points, describing the near steady-state conditions, in order to estimate the experimental steady-state infiltration rate, i_s (mm h^{-1}), and the associated intercept, b_s (mm). Then, the three alternative BEST algorithms were applied to estimate the saturated soil hydraulic conductivity, K_s (mm h^{-1}). θ_s was assumed to coincide with soil porosity, ε (θ_s = ε), as usually suggested by many authors (e.g., Coutinho et al., 2016; Di Prima, 2015; Mubarak et al., 2010; e.g., Xu et al., 2009), since it is not expected to appreciably affect the BEST K_s predictions (Di Prima et al., 2017). For all calculations, the representative PSD, ρ_b, ε, θ_0 and θ_s values of each soil were obtained by averaging the individual determinations (**Table 1**).

2.5. Data analysis

According to the Lilliefors (1967) test, the hypothesis of normal distribution of the untransformed K_s data was not rejected for all the datasets. Therefore, K_s data were assumed to be normally distributed, and were summarized by calculating the mean, and the associated coefficient of variation, CV. Statistical comparison between two sets of data was conducted using a two-tailed t-test, whereas the Tukey Honestly Significant Difference test was applied to compare three or more sets of data. The related p-values were computed and compared to the level of significance of 0.05. Since a fitting of the infiltration model to the transient data is required with BEST-slope and BEST-intercept, the accuracy of these fits were assessed on the basis of the consistency of the model shape and the relative errors, as suggested by (Lassabatere et al., 2006):

$$Er = \sqrt{\frac{\sum_{i=1}^{k}\left[I_{exp}(t_i) - I_{est}(t_i)\right]^2}{\sum_{i=1}^{k} I_{exp}(t_i)^2}} \quad (4)$$

where I_{exp} and I_{est} stand for experimental and estimated values for water infiltration.

3. Results and discussion

3.1. Rainfall simulation experiments and seal characterization

For the RS and RS-T experiments, experimental steady-state runoff rates, *r*, were reached before the end of all runs, so the saturated soil hydraulic conductivity, K_s, values were estimated considering the last data points of the infiltration curves (**Table 2; Figure 3**). For the three studied soils, the mean K_s values of the RS and RS-T experiments ranged from 13.9 to 25.5 and from 15.9 to 26.2 mm h^{-1}, respectively. Visually, the change in soil structure at surface after the simulated storms was evident (**Figure 2**). The compaction of fine material from the destroyed aggregates formed a thin (thickness of ~1 mm) and highly dense seal layer as already observed in previous studies (Assouline, 2004). The impact of rainfall on soil structure looked similar for both RS and RS-T experiments. We then deduced that the bulk densities of the seal layer were comparable for both RS and RS-T experiments. For these last experiments, the soil bulk density increased by 38.7-42.1%, depending on the soil, due to soil surface sealing of the initially undisturbed soils (**Figure 4**).

Di Prima, S., Concialdi, P., Lassabatere, L., Angulo-Jaramillo, R., Pirastru, M., Cerda, A., Keesstra, S., 2018. Laboratory testing of Beerkan infiltration experiments for assessing the role of soil sealing on water infiltration. CATENA 167, 373–384. https://doi.org/10.1016/j.catena.2018.05.013

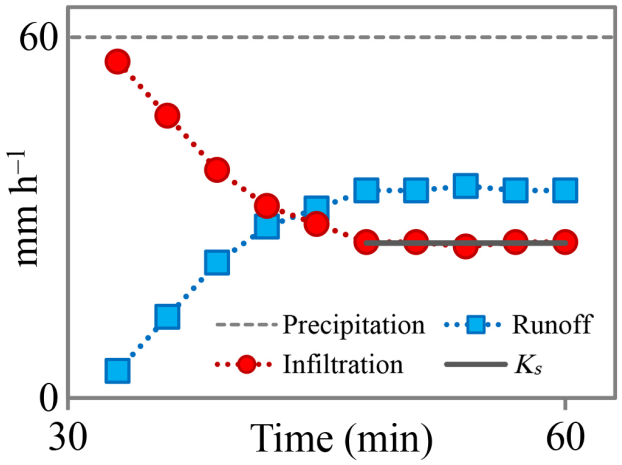

Figure 3. Illustrative example of a simulated rainfall on a sandy-loam plot at 60 mm h^{-1} rainfall intensity. The infiltration curve was drawn by subtracting the runoff rate from the intensity. According to White et al. (1989), the saturated soil hydraulic conductivity, K_s (25.8 mm h^{-1}), was estimated by Eq. (1) considering the last five data points.

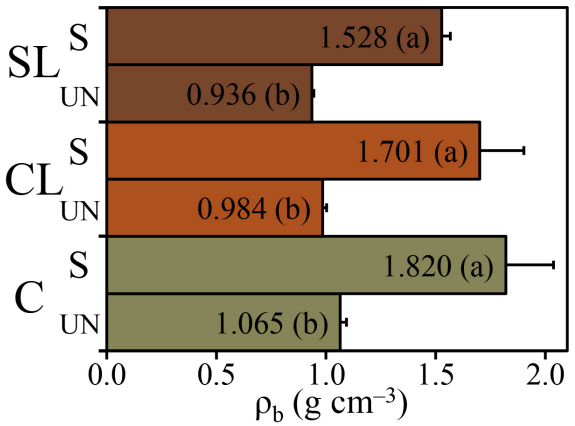

Figure 4. Comparison between the mean bulk density, ρ_b (g cm^{-3}), values of the three undisturbed (UN) soils (sandy-loam, SL, clay-loam, CL, and clay, C) and of the sealed (S) layers sampled after the rainfall simulation experiments carried out on thin soil layers. Bars indicate standard deviation (N = 5). For a given soil, the values followed by a different lower case letter were significantly different according to a two tailed t-test (P < 0.05).

Table 2. Minimum (Min), maximum (Max), mean, and coefficient of variation (CV, in %) of the saturated soil hydraulic conductivity, K_s (mm h^{-1}), values obtained by rainfall simulation experiments carried out on thick (RS) and thin (RS-T) soil layer for the three soils (sandy-loam, SL, clay-loam, CL, and clay, C) (sample size for each method, N = 5).

Site	Method	Min	Max	mean	CV
SL	RS	21.4	31.9	25.5 a	18.1
	RS-T	24.2	27.7	26.2 a	5.4
CL	RS	15.6	22.3	18.8 b	14.0
	RS-T	18.9	21.8	20.8 b	5.9
C	RS	10.6	16.9	13.9 c	21.0
	RS-T	14.9	17.1	15.9 c	6.0

For a given soil, the values followed by the same lower case letter were not significantly different according to a two tailed t-test (P < 0.05). The values followed by a different lower case letter were significantly different.

For each soil, the mean K_s values differed at most by a negligible factor of 1.1 between RS and RS-T experiments, suggesting that considering different soil thicknesses did not appreciably affect the estimated K_s, in terms of average values. A lower variability of K_s was detected with the RS-T experiments, showing that a decrease in the soil thickness implied reduced uncertainties in the estimated mean values of K_s. The statistical irrelevance of the soil thickness on the estimated K_s implied that this parameter was representative of the hydraulic behavior of the least permeable layer (i.e., the seal layer), which controlled the flow at the late-time of the process (Lassabatere et al., 2010). It also suggests that the same type of seal formed with similar saturated hydraulic conductivity, irrespective of the soil thickness. Briefly, water infiltration rates were progressively reduced by the formation of the seal resulting from the direct impact of the drops and tended towards the saturated hydraulic conductivity of the seal at its final stage of development.

3.2. Estimation of K_s of undisturbed soils with BEST algorithms

BEST-L and BEST-H runs obtained for the three undisturbed soils are depicted in **Figure 5**. Experimental cumulative infiltrations clearly show the effect of soil sealing during the course of infiltration experiments. Indeed, the cumulative curves obtained for BEST-H runs follow those obtained for the BEST-L runs before deviating to the right. In other words, infiltration curves have similar concavity for shorter times with a more pronounced concavity for longer times (e.g., **Figure 5**, SL BEST-H versus SL BEST-L, I data). Meanwhile, infiltration rates are comparable for shorter times but differ at longer times with infiltration rates that stabilizes for BEST-L runs whereas infiltration rates continue to decrease for BEST-H runs (e.g. **Figure 5**, SL BEST-H versus SL BEST-L, q data). Cumulative infiltration (I) and infiltration rates (q) obtained for BEST-H runs reveal the impact of soil sealing. At the beginning of experiments, the soil is not sealed at all and water infiltrates into the soil in the same way. Afterwards, when the amount of water applied to soil surface has been enough, the seal begins to form and to impede water infiltration, for BEST H runs. Such impediment reduces water infiltration rates (**Figure 5**, BEST-H runs versus BEST-L runs, q data) and consequently increases the concavity of the cumulative infiltration curve **(Figure 5**, BEST-H runs versus BEST-L runs, I data).

To explain these results, we must consider that BEST procedure assumes the idealized representation of a rigid porous medium (Lassabatere et al., 2013). During a BEST-L run, such condition is reasonably maintained since this procedure is expected to minimize soil surface alteration

Di Prima, S., Concialdi, P., Lassabatere, L., Angulo-Jaramillo, R., Pirastru, M., Cerda, A., Keesstra, S., 2018. Laboratory testing of Beerkan infiltration experiments for assessing the role of soil sealing on water infiltration. CATENA 167, 373–384. https://doi.org/10.1016/j.catena.2018.05.013

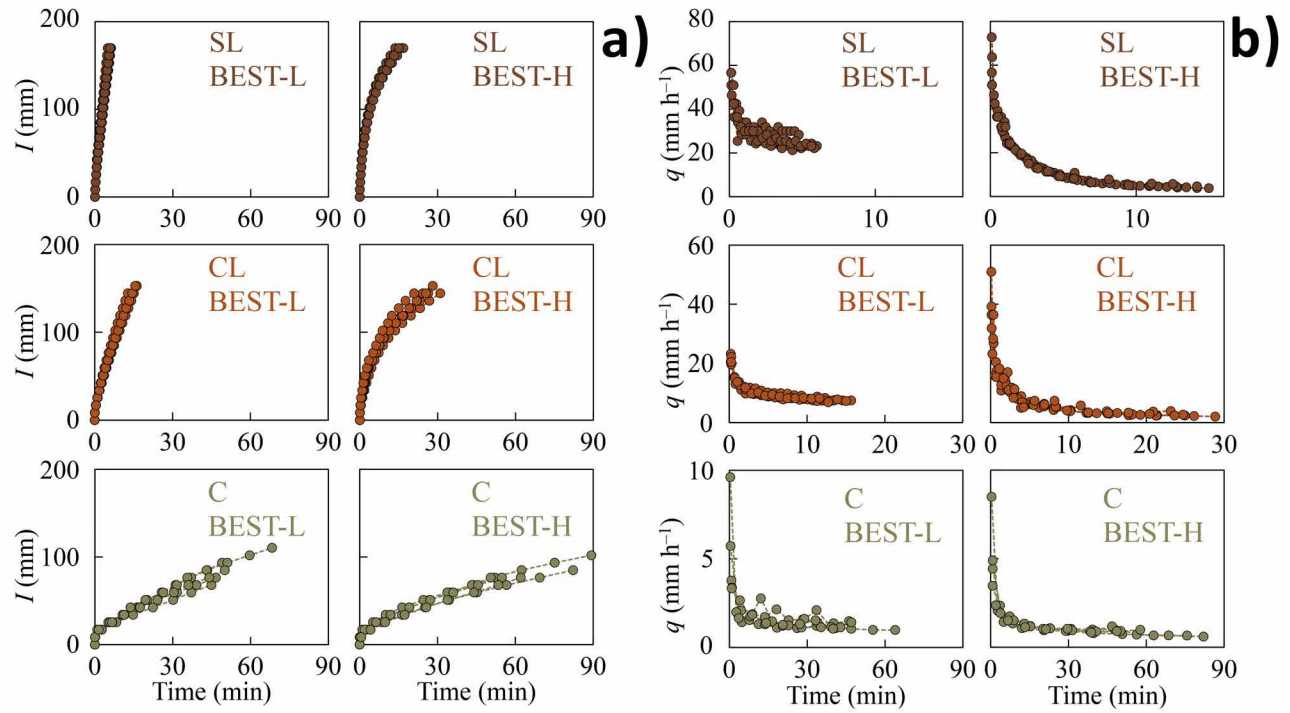

Figure 5. **(a)** Cumulative infiltration, *I* (mm), and **(b)** infiltration rate, *q* (mm h^{-1}), for the three studied soils (sandy-loam, SL, clay-loam, CL, and clay, C) and different heights of water pouring (BEST-L and BEST-H runs).

(Alagna et al., 2016a). Indeed, the structure of the soil is expected not to change appreciably during the experiment, approaching in practice the theoretical assumption of a rigid porous medium. On the other hand, under the exposure to the repeated impact of water volumes falling from a certain height, such as during a BEST-H run, structure dependent soil properties (e.g., hydraulic conductivity) may vary appreciably (Alagna et al., 2016b; Arya et al., 1998; Assouline, 2004; Ben-Hur et al., 2009; Dikinya et al., 2008; Ramos et al., 2000; van De Giesen et al., 2000). During a BEST-H run, the seal is progressively formed at the soil surface by the destruction of the soil aggregates exposed to the direct impact of the poured water volumes (Di Prima et al., 2017). Therefore, it was expected that the dynamic of the seal formation relies on a decrease of saturated hydraulic conductivity of the soil during the exposure to the water drops (Assouline, 2004). As a consequence, the BEST-H runs exhibit a marked concave shape due to the progressive seal formation (**Figure 5**).

The three BEST algorithms were used to treat the BEST-H and BEST-L runs carried out for the three initially unsealed soils. The treatment of the cumulative infiltration data with BEST algorithm may suffer from the impact of soil sealing on curve concavity. In a first step, we discuss the success rates obtained for the three algorithms. The BEST-slope algorithm yielded physically plausible estimates (i.e., positive K_s values) in 16 of 30 infiltration runs (53% of the cases), with the BEST-L procedure showing better results than BEST-H, yielding failure rate values of 7 and 87% respectively. The percentage of successful runs was of 100% with BEST-intercept. However, the fitting of the transient cumulative infiltration model on the data

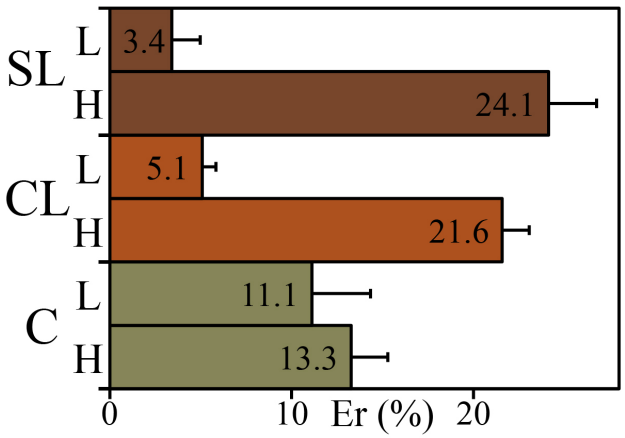

Figure 6. Comparison between the mean relative error, *Er* (%), values (Eq. (4)) of the fitting of the BEST-intercept infiltration model (Eq. (12)) to the transient phase of the infiltration runs for the two heights of water pouring (low, L, and high, H), and for the three studied soils (sandy-loam, SL, clay-loam, CL, and clay, C). Bars indicate standard deviation (*N* = 5).

was less accurate for BEST-H than for BEST-L. With reference to the BEST-L runs, the BEST-intercept algorithm led to acceptable errors *Er* (i.e., $Er \leq 5\%$) for the SL and CL soils. On the other hand, critical *Er* values (i.e., $Er >> 5\%$) were obtained for the BEST-H runs and for both BEST-L and BEST-H runs for the C soil (**Figure 6**).

In addition to this effect on fit errors, soil sealing has also an impact on the quality of estimates for K_s with BEST-slope and BEST-intercept. These algorithms rely on infiltration models, i.e., Eqs. (7b) and Eq. (12), that do not account for such decrease in hydraulic conductivity and related strong curve

Di Prima, S., Concialdi, P., Lassabatere, L., Angulo-Jaramillo, R., Pirastru, M., Cerda, A., Keesstra, S., 2018. Laboratory testing of Beerkan infiltration experiments for assessing the role of soil sealing on water infiltration. CATENA 167, 373–384. https://doi.org/10.1016/j.catena.2018.05.013

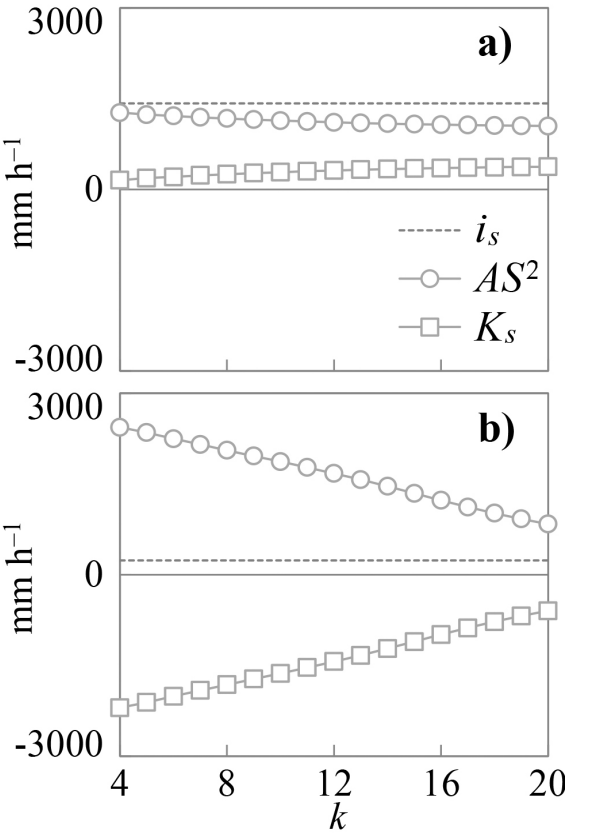

Figure 7. Illustrative example of the estimation of K_s values by Eq. (7a) (BEST-slope) for different number of data points, *k*, **(a)** of a BEST-L run in which the infiltration rate at the end of the experiment (i_s) exceeds the estimated AS^2 values, leading to plausible values for the saturated hydraulic conductivity (positive K_s values), and **(b)** a BEST-H run in which $i_s < AS^2$, leading to erroneous K_s values ($K_s < 0$).

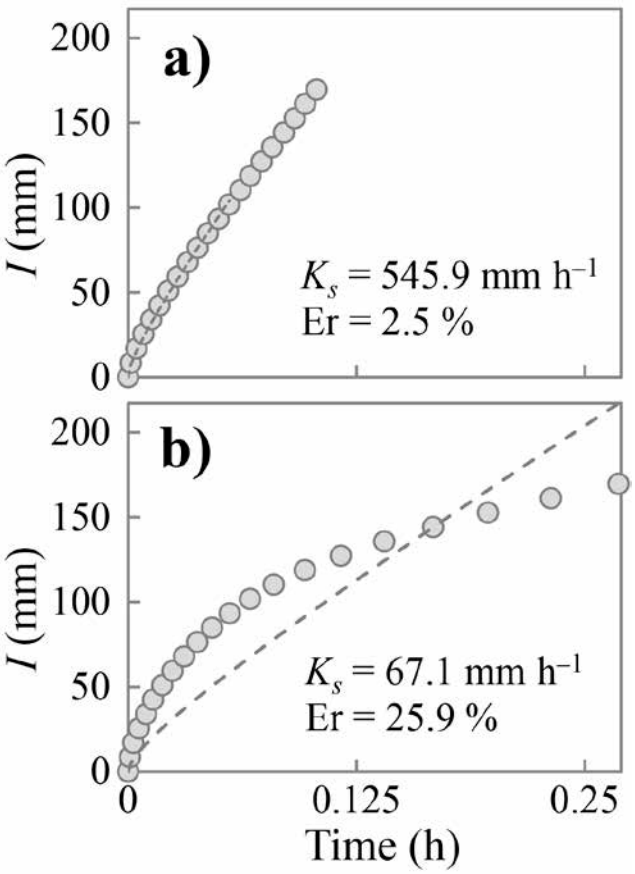

Figure 8. Cumulative infiltration curve **(a)** of a BEST-L run in which Eq. (12) (dotted line; BEST-intercept) fits accordingly to the transient infiltration data yielding an *Er* value smaller than 5%, and **(b)** of a BEST-H run which exhibits a marked concave shape due to the progressive seal formation yielding a poor fit of the infiltration model (*Er* = 25.9 %).

concavity. Therefore, the hydraulic characterization carried out by these algorithms results in miss-estimation and poor performance at the same time. More specifically, the estimation of K_s by Eq. (7a) (BEST-slope) led to negative K_s values with $i_s < AS^2$ (Yilmaz et al., 2010). An illustrative example of K_s misestimation is reported in **Figure 7**. Subpanel **a** depicts the case of a BEST-L run and the proper estimation of the K_s values by Eq. (7a). In this case the infiltration rate at the end of the experiment exceeds the estimated AS^2 values, leading to physically plausible and positive values for the saturated hydraulic conductivity. On the contrary, when the early- and late-time infiltration stages greatly differ in terms of infiltration rates as the result of the seal formation, the strong concavity of cumulative infiltration results in an over-estimation of soil sorptivity. Such overestimation results in too large values for the term AS^2 in Eq. (7a), resulting in negative values for K_s (Figure 7b).

For the case of the BEST-H runs analyzed with the BEST-intercept algorithm the main problem was related to the poor fitting performance of the infiltration model with relative errors exceeding 5% (**Figure 6**). **Figure 8a** depicts the cumulative infiltration curve of a BEST-L run in which the infiltration model (Eq. (12)) fits accordingly to the transient infiltration data. Indeed, in this case the cumulative infiltration curve exhibits an usual shape, i.e., a gently concave part corresponding to the transient state and a linear part at the end of the curves related to the steady state (Di Prima et al., 2016). In the second case (**Figure 8b**), the cumulative infiltration of the BEST-H run exhibits a marked concave shape due to the progressive seal formation. The marked concavity cannot be properly modelled by the infiltration model; which yields a poor fit of the infiltration model with a large value for relative error (*Er* = 25.9%).

The inadaptability of BEST procedure to characterize sealed soils does not necessary occur if the seal is characterized a posteriori, i.e., once it is completely formed. For instance, Alagna et al. (in press) analyzed with the BEST-slope algorithm infiltration runs carried out using the BEST-L procedure on a crusted loamy soil in a Mediterranean vineyard (western Sicily, Italy). BEST-slope yielded positive K_s values in all cases. In addition, Eq. (7b) always yielded accurate fits with low relative errors. These authors concluded that the derived BEST-slope parameters were representative of the hydraulic behavior of the least permeable layer (i.e., the crust layer), which

Di Prima, S., Concialdi, P., Lassabatere, L., Angulo-Jaramillo, R., Pirastru, M., Cerda, A., Keesstra, S., 2018. Laboratory testing of Beerkan infiltration experiments for assessing the role of soil sealing on water infiltration. CATENA 167, 373–384. https://doi.org/10.1016/j.catena.2018.05.013

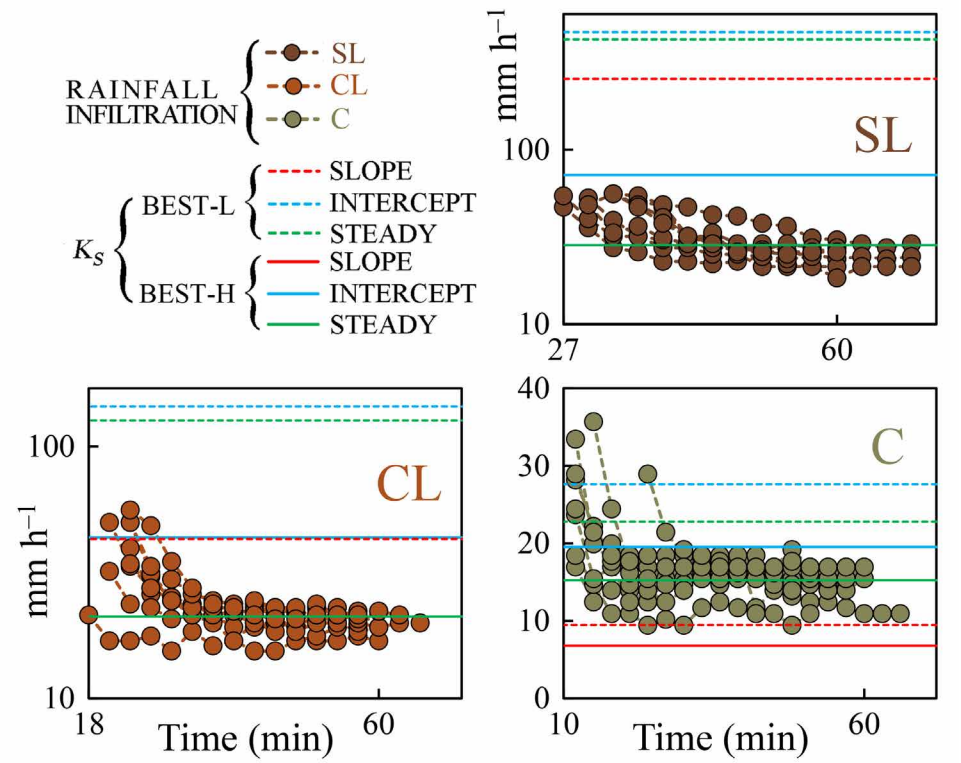

Figure 9. Comparison between the mean K_s values obtained by the three BEST algorithms (BEST-slope, BEST-intercept and BEST-steady) and pouring water into the cylinder from two different heights (BEST-L and BEST-H runs), and infiltration rates of the rainfall simulation experiments for the three soils (sandy-loam, SL, clay-loam, CL, and clay, C).

controlled the flow and consequently cumulative infiltration of the stratified medium, as proposed by Lassabatere et al. (2010) for layered soils.

Lastly, BEST-steady algorithm led to plausible values in 100% of the cases, thus proving more robust and efficient results than the other two BEST algorithms. However, even if BEST-steady appeared to be more robust than the other algorithms, additional information is needed to confirm that the target soil hydraulic parameters were accurately estimated. To overcome this lack, in the following section a comparison with independent K_s data estimated by rainfall simulation experiments was done in order to assess the adequacy of the three BEST algorithms.

We reported the averages of all the plausible estimates for both BEST-L and BEST-H runs for the three undisturbed soils in **Table 3**. As already discussed, BEST-H runs analyzed with the BEST-slope algorithm yielded a very high failure rate, leading to no values for SL and CL soils. BEST-intercept yielded poor fits and probably misestimated or overestimated values for K_s for the same soils and BEST-H runs (values highlighted in **Table 3**). In opposite, the case of BEST-L runs lead to proper BEST modelling and estimates. The comparison between BEST-H and BEST-L runs shows a significant decrease in K_s estimates from L to H. The height of water pouring had a strong impact with a clear decrease in estimates for K_s, probably due to seal formation during BEST-H runs.

The situation was different for the C soil. The discrepancy of BEST models and related erroneous values was less significant. For instance, estimates could be obtained with BEST-slope algorithm in all cases. The difference of height of water pouring did not yield a clear difference between BEST-L and BEST-H runs. Mean K_s values ranged between 6.8 and 27.6 mm h^{-1}. Differences between the two procedures were less noticeable than the other soils, with the BEST-L runs yielding higher means than BEST-H by a factor 1.4-1.5, depending on the algorithm. Such difference can be considered practically negligible for many hydrological applications (Elrick and Reynolds, 1992). We conclude that C soil showed a higher susceptibility to sealing in all cases (confirmed also by visual information), even if precautions were taken to minimize soil alteration (BEST-L runs). The susceptibility of this soil is not surprising, given its low organic matter content (1.1%) and the related absence of aggregates and soil structure (Reynolds et al., 2009). In addition, for this soil, clay dispersion is a possible additional mechanism responsible for the reduction of the hydraulic conductivity of saturated or near-saturated soil upon wetting (Bagarello et al., 2006).

3.3. Comparing K_s data estimated by contrasting infiltration techniques

In **Figure 9**, all the infiltration rates obtained during the rainfall experiments are plotted against time. The data obtained for both the soil thickness (RS and RS-T experiments) were considered given the similarity of the collected experimental information in the two cases. The values of K_s

Di Prima, S., Concialdi, P., Lassabatere, L., Angulo-Jaramillo, R., Pirastru, M., Cerda, A., Keesstra, S., 2018. Laboratory testing of Beerkan infiltration experiments for assessing the role of soil sealing on water infiltration. CATENA 167, 373–384. https://doi.org/10.1016/j.catena.2018.05.013

Table 3. Sample size, N, minimum, Min, maximum, Max, mean, and coefficient of variation, CV (%), of saturated soil hydraulic conductivity, K_s (mm h^{-1}), values obtained by the three BEST algorithms and low and high height of water pouring for the three soils (sandy-loam, SL, clay-loam, CL, and clay, C).

Soil	Height of water pouring	BEST algorithm	Statistic				
			N	Min	Max	mean	CV
SL	High	slope			$K_s < 0$		
		intercept	5	64.8	78.7	71.7	8.5
		steady	5	24.7	36.1	28.4	17.6
	Low	slope	5	76.7	404.3	255.4	52.6
		intercept	5	392.0	598.8	473.2	19.7
		steady	5	343.8	553.5	430.2	20.8
CL	High	slope			$K_s < 0$		
		intercept	5	36.8	51.1	43.5	11.7
		steady	5	18.2	23.3	21.1	9.2
	Low	slope	5	17.7	66.7	43.0	45.7
		intercept	5	135.6	156.4	144.1	6.2
		steady	5	116.5	136.4	126.8	6.8
C	High	slope	2	0.8	12.8	6.8	125.6
		intercept	5	12.0	26.0	19.5	31.2
		steady	5	7.6	22.1	15.2	39.2
	Low	slope	4	2.8	17.0	9.5	65.7
		intercept	5	17.5	33.5	27.6	22.6
		steady	5	12.5	28.3	22.8	27.9

The underlined values indicated mean K_s values calculated with wrong estimations and unacceptable values for fit relative errors.

obtained for the soils with BEST-H and BEST-L runs and for the three BEST algorithms are depicted on the same graph. As shown in **Figure 9**, for the SL and CL soils, only the BEST-H procedure along with the BEST-steady algorithm yielded similar K_s values with those obtained by the rainfall simulation experiments. K_s values provided by BEST-L runs were much higher and inconsistent with RS and RS-T infiltration rates for soils SL and CL. Such discrepancy results from the absence of soil sealing for BEST-L runs and from the fact the K_s of undisturbed soils are much higher than that of the seal. For soil C, the difference for K_s estimates between BEST-L and BEST-H runs is less important. For the three soils, the estimates of K_s that are the most consistent with RS and RS-T infiltration rates are those obtained with BEST-H runs with BEST-steady algorithm. BEST-intercept and -slope lead to less consistent values. Note that BEST-provided no value for BEST-H runs and soils SL and CL (avoiding any comparison).

The result obtained with reference to the height of water pouring can be viewed as a confirmation of previous investigations (Alagna et al., 2016a; Bagarello et al., 2014a, 2017; Di Prima et al., 2017). More specifically, as already outlined by Di Prima et al. (2017), K_s data collected by ponding infiltrometer methods and usual experimental procedures, such as BEST-L runs, are generally expected to be unusable for interpreting field hydrological processes and particularly rainfall infiltration on bare soils prone to sealing. On the contrary, both rainfall simulation experiments and the BEST-H procedure determine a certain degree of compaction and mechanical breakdown of aggregates, accurately simulating processes during intense rainfall events. Therefore, K_s values estimated by these latter methodologies are more appropriate to explain surface runoff generation phenomena during intense storms.

A further objective of this investigation was to understand which BEST algorithm among BEST-slope, -intercept and -steady can be satisfactorily selected to properly estimate K_s for the specific case of an infiltration experiment implying an alteration of the soil surface. The K_s comparison carried out by applying different procedures to analyze the same infiltration run and independent rainfall simulation experiments allowed to identify BEST-steady as the most appropriate algorithm to estimate hydraulic properties from the BEST-H runs (**Figure 9**). The statistical comparison reported in **Figure 10** supported the hypothesis that a characterization made with BEST-steady could be more appropriate to determine K_s data at the advanced stage of the seal formation of an initially undisturbed bare soil. Indeed, no statistical differences were detected between the mean K_s values obtained by the BEST-H procedure along with BEST-steady algorithm and by the rainfall simulation experiments. This result likely depends on the fact that BEST-steady considers exclusively the late phase of the infiltration process, i.e., when the seal is fully developed. Limiting the hydraulic characterization to the stabilized phase avoids the uncertainties due to specific shape of the cumulative infiltration and a no clear distinction between the early- and late-time infiltration process because of the progressive alteration of the soil surface (Bagarello et al., 2014b). Another implication of this result was that, with both methods, the formed seal layer ruled the late phase of the infiltration process and the estimated K_s values were representative of the seal (**Figure 10**). In other words, the experiments presented in this study suggest that if any seal forms at the surface during a BEST-H infiltration test the BEST-steady estimates should proper characterize the hydraulic properties of the seal. We believe that this result has practical importance because, to our

Di Prima, S., Concialdi, P., Lassabatere, L., Angulo-Jaramillo, R., Pirastru, M., Cerda, A., Keesstra, S., 2018. Laboratory testing of Beerkan infiltration experiments for assessing the role of soil sealing on water infiltration. CATENA 167, 373–384. https://doi.org/10.1016/j.catena.2018.05.013

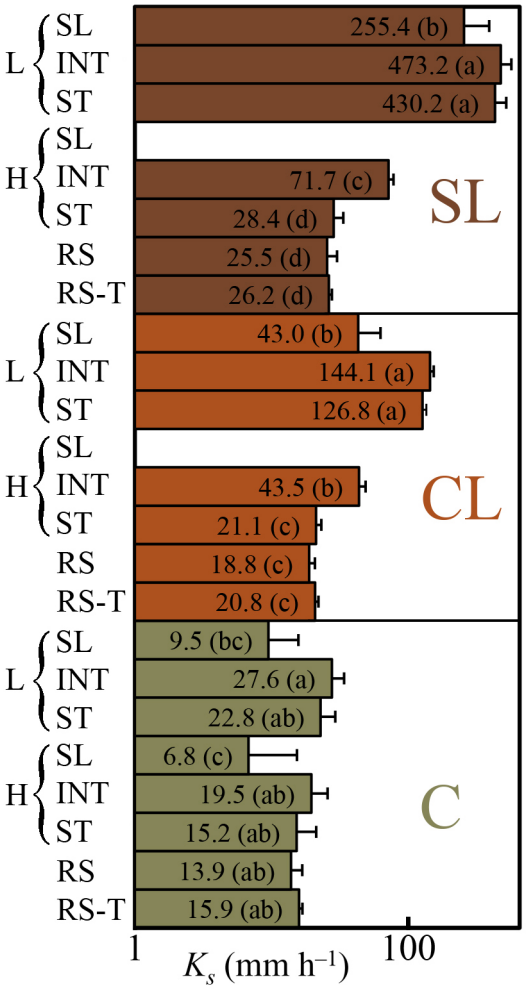

Figure 10. Comparison between the mean K_s values obtained by the three BEST algorithms (BEST-slope, SL, BEST-intercept, INT, and BEST-steady, ST) and pouring water into the cylinder from two different heights (BEST-L, L, and BEST-H, H, runs) and by the rainfall simulation experiments carried out on thick (RS) and thin (RS-T) soil layer for the three soils (sandy-loam, SL, clay-loam, CL, and clay, C). Bars indicate standard deviation (N = 5). For a given soil, the values followed by the same lower case letter were not significantly different according to the Tukey Honestly Significant Difference test (P < 0.05). The values followed by a different lower case letter were significantly different.

knowledge, this was the first time that a check of the BEST-H procedure and the three BEST algorithms with other well tested methods for K_s estimation was carried out to characterize sealing at the surface of several types of soils.

4. Summary and conclusions

In this study, we firstly used rainfall simulations to assess the effect of soil sealing on infiltration of three initially undisturbed bare soils with different textures, Clay, Clay Loam and Sandy Loam over a layer of sand. A system with the thickness of soil corresponding to the seal thickness (~2 mm) was tested versus 75 mm thickness for the upper soil layer. The results clearly pointed at similar processes and results for the large and small thickness of the upper layer. The formation of the seal appeared identical, irrespective of the upper layer thickness. The experimental data showed that soil sealing determined an increase in soil bulk density varying from 38.7 to 42.1%, depending on the soil. Such a decrease resulted in a significant drop in hydraulic conductivity with time. Water infiltration was governed mainly by seal formation and related decrease in saturated hydraulic conductivity. Under the conditions simulated here, the final infiltration rates were representative of the hydraulic behavior of the seal layer, which controlled the infiltration process at the late-phase of the rainfall simulations, irrespective of the upper soil layer thickness.

The potential of the BEST-H procedure, to simulate and assess the alteration of the soil surface, was then tested in conjunction with the three existing BEST algorithms, i.e., BEST-slope, BEST-intercept and BEST-steady, to derive saturated hydraulic conductivity. For each soil, the potential of the BEST-H procedure was tested comparing the K_s estimates with the corresponding target values, i.e., the K_s values estimated by rainfall simulation experiments. Among the existing BEST algorithms, BEST-steady allowed a proper estimation of K_s for all the studied soils. More specifically, this algorithm limited the hydraulic characterization to the stabilized phase, i.e., when the seal was fully developed, avoiding uncertainties due to the seal formation during the early phase of the infiltration process. The other two algorithms that account for transient data are too perturbed by the effect of the progressive formation of the seal and related impacts on the infiltration. BEST-H runs along with BEST-steady algorithm prove more appropriate for the characterization of sealed soils and the hydraulic conductivity of the seal. These low-cost techniques may be advantageous in comparison with more intensive techniques like rainfall simulations experiments.

Our findings demonstrated that the BEST-H procedure is suitable enough to properly characterize the seal layer formed during the repeated impact of the poured water volumes onto the initially unsealed soil surface. The repeated impact of water drops during a BEST-H run induced the formation of a seal layer having similar hydraulic properties with those obtained by the simulated storms. In other terms, the BEST-H runs had possibly accounted for the main physical features characterizing the phenomenon of induced soil sealing. We propose that the applied methodology here could be adopted as a simple tool in investigations aimed to study the impact of sealing on soil infiltration in situ and in the laboratory, particularly to explain surface runoff generation phenomena during intense storms, quantifying soil susceptibility to erosion, or investigating the effect of soil restoration strategies to improve the soil properties (Badalamenti et al., 2016; Pasta et al., 2012).

These findings also have direct implications in terms of our understanding of land management. The infiltration is determined by the first few millimeters of the soil. This shows the importance of soil surface management for the functioning of the soil in terms of the partitioning of the rainfall into

Di Prima, S., Concialdi, P., Lassabatere, L., Angulo-Jaramillo, R., Pirastru, M., Cerda, A., Keesstra, S., 2018. Laboratory testing of Beerkan infiltration experiments for assessing the role of soil sealing on water infiltration. CATENA 167, 373–384. https://doi.org/10.1016/j.catena.2018.05.013

infiltration and runoff, as well as the associated soil erosion and the movement of sediment and associated substances through the landscape. In the future, the proposed methodology may be applied for different rainfall intensities and durations. Indeed, rainfall characteristics are among the major factors affecting the dynamics of seal formation.

Acknowledgements

We acknowledge the Earth System Science and Environmental Management (ESSEM) COST Action ES1306 "Connecting European connectivity research" for the scholarship grant awarded to S. Di Prima. P. Concialdi helped to run the Beerkan infiltration experiments. S. Di Prima outlined the investigation, designed the rainfall box, performed the rainfall simulation experiments and analyzed the data. All authors contributed to discuss the results and write the manuscript. S.D.P. also thank H.M., P.R. and F.P.

Appendix A

For an infiltration experiment with zero pressure head on a circular surface of radius r_d (mm), the three-dimensional cumulative infiltration, I (mm), and infiltration rate, i (mm h^{-1}), can be approached by the following explicit transient [Eqs.(5a) and (5b)] and steady-state [Eqs.(5c) and (5d)] expansions (Haverkamp et al., 1994; Lassabatere et al., 2006):

$$I(t) = S\sqrt{t} + \left(AS^2 + BK_s\right) t \quad (5a)$$

$$i(t) = \frac{S}{2\sqrt{t}} + \left(AS^2 + BK_s\right) \quad (5b)$$

$$I_{+\infty}(t) = \left(AS^2 + K_s\right) t + C\frac{S^2}{K_s} \quad (5c)$$

$$i_s = AS^2 + K_s \quad (5d)$$

where t (h) is the time, S (mm $h^{-1/2}$) is soil sorptivity, and A (mm^{-1}), B and C are constants defined taking into account initial conditions as (Haverkamp et al., 1994):

$$A = \frac{\gamma}{r_d\left(\theta_s - \theta_0\right)} \quad (6a)$$

$$B = \frac{2-\beta}{3}\left[1 - \left(\frac{\theta_0}{\theta_s}\right)^{\eta}\right] + \left(\frac{\theta_0}{\theta_s}\right)^{\eta} \quad (6b)$$

$$C = \frac{1}{2\left[1 - \left(\frac{\theta_0}{\theta_s}\right)^{\eta}\right](1-\beta)} In\left(\frac{1}{\beta}\right) \quad (6c)$$

Where θ_0 (cm^3cm^{-3}) is the initial volumetric water content, γ is parameter for geometrical correction of the infiltration front shape (Castellini et al., 2018), and β is a parameter depending on the capillary diffusivity function (Angulo-Jaramillo et al., 2000). γ and β are commonly set at 0.75 and 0.6 for $\theta_0 < 0.25\ \theta_s$ (Haverkamp et al., 1994). Note that relations (6) apply only when residual water content is negligible and that these equations are sensitive to the estimation of saturated water content, which may be quite challenging under specific circumstances (Di Prima et al., 2017).

The three alternative BEST algorithms differ from the way they fit experimental data to the models defined by Eq. (5a). In particular, a fitting of the infiltration model to the transient data is required with BEST-slope and BEST-intercept, but these differ by the use of steady-state conditions described by i_s for the former algorithm and b_s for the latter one. Both of these last two terms are required by BEST-steady that does not need data fitting to the transient stage of the run but relies solely on the steady state. In the following, are presented the detailed descriptions of the three alternative BEST algorithms.

The BEST-slope algorithm by Lassabatère et al. (2006) considers Eq. (5a) for modelling the transient cumulative infiltration data. Eq. (5a) is modified with the replacement of hydraulic conductivity as a function of sorptivity and the experimental steady-state infiltration rate, i_s, using Eq. (5d), leading to:

$$K_s = i_s - AS^2 \quad (7a)$$

$$I(t) = S\sqrt{t} + \left[A(1-B)S^2 + B\ i_s\right] t \quad (7b)$$

where i_s is estimated as the slope of regression line fitted to the last data points describing the steady-state conditions on the I vs. t plot. Eq. (7b) is fitted to experimental data to estimate S. Establishing a constraint like Eq. (7a) between the estimator for sorptivity and the one for saturated hydraulic conductivity and inverting cumulative infiltration data through optimizing only sorptivity avoids parameter non-uniqueness and increases the robustness of the inverse procedure (Lassabatere et al., 2013). The fit is performed by minimizing the classical objective function for cumulative infiltration:

$$f\left(S,\ K_s,\ k\right) = \sum_{i=1}^{k}\left[I_{exp}(t_i) - I_{est}(t_i)\right]^2 \quad (8)$$

where k is the number of data points considered for the transient state, I_{exp} is the experimental cumulative infiltration and I_{est} is the estimated cumulative infiltration using Eq. (7b). Once S is estimated, K_s is calculated by Eq. (7a). As the infiltration model is valid only at transient state, the fit may not be valid for large values of k. Therefore, BEST fits data for a minimum of two points to a maximum of N_{tot} points,

Di Prima, S., Concialdi, P., Lassabatere, L., Angulo-Jaramillo, R., Pirastru, M., Cerda, A., Keesstra, S., 2018. Laboratory testing of Beerkan infiltration experiments for assessing the role of soil sealing on water infiltration. CATENA 167, 373–384. https://doi.org/10.1016/j.catena.2018.05.013

representing the whole dataset. For each data subset containing the first k points, corresponding to a duration of the experiment equal to t_k, S and K_s are estimated and the time, t_{max} (h), defined as the maximum time for which the transient expression can be considered valid, is determined as follow:

$$t_{max} = \frac{1}{4(1-B)^2}\left(\frac{S}{K_s}\right)^2 \quad (9)$$

where $(S/K_s)^2$ is the gravity time defined by Philip (1969). Then, t_k is compared with t_{max}. The values of S and K_s are not considered valid unless t_k is lower than t_{max}. Among all values of S and K_s that fulfill this condition, the S and K_s values corresponding to the largest k (k_{step}) are retained since they are considered more precise.

The BEST-intercept algorithm by Yilmaz et al. (2010) defines the constraint between S and K_s by using the intercept of the asymptotic expansion in Eq. (5c):

$$b_s = \frac{C\ S^2}{K_s} \quad (10)$$

Therefore, b_s is estimated by linear regression analysis of the data describing steady-state conditions on the I vs. t plot, and the following relationship is applied to determine K_s:

$$K_s = C\frac{S^2}{b_s} \quad (11)$$

This procedure leads to the use of the division operator rather than the subtraction operator and thereby avoids obtaining negative values for the estimation of K_s. Combining Eqs. (5a) and (11) yields the following relationship to fit onto the transient state of the experimental cumulative infiltration:

$$I(t) = S\sqrt{t} + \left(AS^2 + BC\frac{S^2}{b_s}\right)t \quad (12)$$

Eq. (12), that is alternative to Eq. (7b), is applied to determine S by the same procedure described for BEST-slope, including the assessment of the time validity of the transient infiltration model by calculation of t_{max}. The estimated sorptivity is then used to calculate K_s by Eq. (11).

Finally, the BEST-steady procedure by Bagarello et al. (2014b) makes use of both the intercept (b_s) and the slope (i_s) of the straight line fitted to the data describing steady-state conditions on the I vs. t plot. With this algorithm K_s can be directly calculated by the following equation (Di Prima et al., 2016):

$$K_s = \frac{C\ i_s}{A\ b_s + C} \quad (13)$$

Finally, the scale parameter for water pressure head can be computed from previous estimates of saturated hydraulic conductivity and sorptivity (Lassabatere et al., 2006). However, in this study, we focus mainly on the value of saturated hydraulic conductivity, K_s.

References

Alagna, V., Bagarello, V., Di Prima, S., Giordano, G., Iovino, M., 2016a. Testing infiltration run effects on the estimated water transmission properties of a sandy-loam soil. Geoderma 267, 24–33. https://doi.org/10.1016/j.geoderma.2015.12.029

Alagna, V., Bagarello, V., Di Prima, S., Giordano, G., Iovino, M., 2013. A simple field method to measure the hydrodynamic properties of soil surface crust. Journal of Agricultural Engineering 44, 74–79. https://doi.org/10.4081/jae.2013.(s1):e14

Alagna, V., Bagarello, V., Di Prima, S., Guaitoli, F., Iovino, M., Keesstra, S., Cerdà, A., 2019. Using beerkan experiments to estimate hydraulic conductivity of a crusted loamy soil in a Mediterranean vineyard. Journal of Hydrology and Hydromechanics 67.

Alagna, V., Bagarello, V., Di Prima, S., Iovino, M., 2016b. Determining hydraulic properties of a loam soil by alternative infiltrometer techniques. Hydrological Processes 30, 263–275. https://doi.org/10.1002/hyp.10607

Alagna, V., Di Prima, S., Rodrigo-Comino, J., Iovino, M., Pirastru, M., Keesstra, S.D., Novara, A., Cerdà, A., 2017. The Impact of the Age of Vines on Soil Hydraulic Conductivity in Vineyards in Eastern Spain. Water 10, 14. https://doi.org/10.3390/w10010014

Angulo-Jaramillo, R., Bagarello, V., Iovino, M., Lassabatère, L., 2016. Infiltration Measurements for Soil Hydraulic Characterization. Springer International Publishing.

Angulo-Jaramillo, R., Vandervaere, J.-P., Roulier, S., Thony, J.-L., Gaudet, J.-P., Vauclin, M., 2000. Field measurement of soil surface hydraulic properties by disc and ring infiltrometers: A review and recent developments. Soil and Tillage Research 55, 1–29. https://doi.org/10.1016/S0167-1987(00)00098-2

Arya, L.M., Dierolf, T.S., Sofyan, A., Widjaja-Adhi, I., van Genuchten, M.T., 1998. Field measurement of the saturated hydraulic conductivity of a macroporous soil with unstable subsoil structure. Soil science 163, 841–852.

Assouline, S., 2004. Rainfall-induced soil surface sealing. Vadose Zone Journal 3, 570–591.

Assouline, S., Mualem, Y., 2002. Infiltration during soil sealing: The effect of areal heterogeneity of soil hydraulic properties. Water Resources Research 38, 1286. https://doi.org/10.1029/2001WR001168

Augeard, B., Assouline, S., Fonty, A., Kao, C., Vauclin, M., 2007. Estimating hydraulic properties of rainfall-induced soil surface seals from infiltration experiments and X-ray bulk density measurements. Journal of Hydrology 341, 12–26. https://doi.org/10.1016/j.jhydrol.2007.04.018

Badalamenti, E., Gristina, L., Laudicina, V.A., Novara, A., Pasta, S., Mantia, T.L., 2016. The impact of Carpobrotus cfr. acinaciformis (L.) L. Bolus on soil nutrients, microbial communities structure and native plant communities in Mediterranean ecosystems. Plant Soil 409, 19–34. https://doi.org/10.1007/s11104-016-2924-z

Bagarello, V., Castellini, M., Di Prima, S., Iovino, M., 2014a. Soil hydraulic properties determined by infiltration experiments and different heights of water pouring. Geoderma 213, 492–501. https://doi.org/10.1016/j.geoderma.2013.08.032

Bagarello, V., Cecere, N., Di Prima, S., Giordano, G., Iovino, M., 2017. Height of water pouring effects on infiltration runs carried out in an

initially wet sandy-loam soil, in: Chemical Engineering Transactions, Chemical Engineering Transactions. Italian Association of Chemical Engineering - AIDIC, pp. 721–726. https://doi.org/10.3303/cet1758121
Bagarello, V., Di Prima, S., Iovino, M., 2014b. Comparing Alternative Algorithms to Analyze the Beerkan Infiltration Experiment. Soil Science Society of America Journal 78, 724. https://doi.org/10.2136/sssaj2013.06.0231
Bagarello, V., Di Prima, S., Iovino, M., Provenzano, G., Sgroi, A., 2011. Testing different approaches to characterize Burundian soils by the BEST procedure. Geoderma 162, 141–150. https://doi.org/10.1016/j.geoderma.2011.01.014
Bagarello, V., Iovino, M., Palazzolo, E., Panno, M., Reynolds, W.D., 2006. Field and laboratory approaches for determining sodicity effects on saturated soil hydraulic conductivity. Geoderma 130, 1–13. https://doi.org/10.1016/j.geoderma.2005.01.004
Baumhardt, R.L., Römkens, M.J.M., Whisler, F.D., Parlange, J.-Y., 1990. Modeling infiltration into a sealing soil. Water Resour. Res. 26, 2497–2505. https://doi.org/10.1029/WR026i010p02497
Ben-Hur, M., Yolcu, G., Uysal, H., Lado, M., Paz, A., 2009. Soil structure changes: aggregate size and soil texture effects on hydraulic conductivity under different saline and sodic conditions. Aust. J. Soil Res. 47, 688–696.
Bradford, J.M., Ferris, J.E., Remley, P.A., 1987. Interrill soil erosion processes: I. Effect of surface sealing on infiltration, runoff, and soil splash detachment. Soil Science Society of America Journal 51, 1566–1571.
Braud, I., De Condappa, D., Soria, J.M., Haverkamp, R., Angulo-Jaramillo, R., Galle, S., Vauclin, M., 2005. Use of scaled forms of the infiltration equation for the estimation of unsaturated soil hydraulic properties (the Beerkan method). European Journal of Soil Science 56, 361–374. https://doi.org/10.1111/j.1365-2389.2004.00660.x
Brooks, R.H., Corey, T., 1964. hydraulic properties of porous media. Hydrol. Paper 3., Colorado State University, Fort Collins.
Burdine, N.T., 1953. Relative permeability calculation from pore size distribution data. Petr. Trans.AmInst. Min. Metall. Eng. 198, 71–77.
Castellini, M., Di Prima, S., Iovino, M., 2018. An assessment of the BEST procedure to estimate the soil water retention curve: A comparison with the evaporation method. Geoderma 320, 82–94. https://doi.org/10.1016/j.geoderma.2018.01.014
Coutinho, A.P., Lassabatere, L., Montenegro, S., Antonino, A.C.D., Angulo-Jaramillo, R., Cabral, J.J.S.P., 2016. Hydraulic characterization and hydrological behaviour of a pilot permeable pavement in an urban centre, Brazil. Hydrol. Process. 30, 4242–4254. https://doi.org/10.1002/hyp.10985
Di Prima, S., 2015. Automated single ring infiltrometer with a low-cost microcontroller circuit. Computers and Electronics in Agriculture 118, 390–395. https://doi.org/10.1016/j.compag.2015.09.022
Di Prima, S., Bagarello, V., Lassabatere, L., Angulo-Jaramillo, R., Bautista, I., Burguet, M., Cerdà, A., Iovino, M., Prosdocimi, M., 2017. Comparing Beerkan infiltration tests with rainfall simulation experiments for hydraulic characterization of a sandy-loam soil. Hydrological Processes 31, 3520–3532. https://doi.org/10.1002/hyp.11273
Di Prima, S., Lassabatere, L., Bagarello, V., Iovino, M., Angulo-Jaramillo, R., 2016. Testing a new automated single ring infiltrometer for Beerkan infiltration experiments. Geoderma 262, 20–34. https://doi.org/10.1016/j.geoderma.2015.08.006
Dikinya, O., Hinz, C., Aylmore, G., 2008. Decrease in hydraulic conductivity and particle release associated with self-filtration in saturated soil columns. Geoderma 146, 192–200. https://doi.org/10.1016/j.geoderma.2008.05.014
Elrick, D.E., Reynolds, W.D., 1992. Methods for analyzing constant-head well permeameter data. Soil Science Society of America Journal 56, 320. https://doi.org/10.2136/sssaj1992.03615995005600010052x
Fernández-Raga, M., Palencia, C., Keesstra, S., Jordán, A., Fraile, R., Angulo-Martínez, M., Cerdà, A., 2017. Splash erosion: A review with unanswered questions. Earth-Science Reviews 171, 463–477. https://doi.org/10.1016/j.earscirev.2017.06.009
Gee, G.W., Bauder, J.W., 1986. Particle-size Analysis, in: SSSA Book Series, Klute, A. (Ed.), Methods of Soil Analysis, Part 1: Physical and Mineralogical Methods. Soil Science Society of America, American Society of Agronomy, pp. 383–411.
Gonzalez-Sosa, E., Braud, I., Dehotin, J., Lassabatère, L., Angulo-Jaramillo, R., Lagouy, M., Branger, F., Jacqueminet, C., Kermadi, S., Michel, K., 2010. Impact of land use on the hydraulic properties of the topsoil in a small French catchment. Hydrol. Process. 24, 2382–2399. https://doi.org/10.1002/hyp.7640
Haverkamp, R., Ross, P.J., Smettem, K.R.J., Parlange, J.Y., 1994. Three-dimensional analysis of infiltration from the disc infiltrometer: 2. Physically based infiltration equation. Water Resour. Res. 30, 2931–2935. https://doi.org/10.1029/94WR01788
Iserloh, T., Ries, J.B., Arnáez, J., Boix-Fayos, C., Butzen, V., Cerdà, A., Echeverría, M.T., Fernández-Gálvez, J., Fister, W., Geißler, C., Gómez, J.A., Gómez-Macpherson, H., Kuhn, N.J., Lázaro, R., León, F.J., Martínez-Mena, M., Martínez-Murillo, J.F., Marzen, M., Mingorance, M.D., Ortigosa, L., Peters, P., Regüés, D., Ruiz-Sinoga, J.D., Scholten, T., Seeger, M., Solé-Benet, A., Wengel, R., Wirtz, S., 2013. European small portable rainfall simulators: A comparison of rainfall characteristics. CATENA 110, 100–112. https://doi.org/10.1016/j.catena.2013.05.013
Lado, M., Ben-Hur, M., Shainberg, I., 2004. Soil Wetting and Texture Effects on Aggregate Stability, Seal Formation, and Erosion. Soil Science Society of America Journal 68, 1992–1999. https://doi.org/10.2136/sssaj2004.1992
Lassabatere, L., Angulo-Jaramillo, R., Goutaland, D., Letellier, L., Gaudet, J.P., Winiarski, T., Delolme, C., 2010. Effect of the settlement of sediments on water infiltration in two urban infiltration basins. Geoderma 156, 316–325. https://doi.org/10.1016/j.geoderma.2010.02.031
Lassabatere, L., Angulo-Jaramillo, R., Soria Ugalde, J.M., Cuenca, R., Braud, I., Haverkamp, R., 2006. Beerkan estimation of soil transfer parameters through infiltration experiments—BEST. Soil Science Society of America Journal 70, 521. https://doi.org/10.2136/sssaj2005.0026
Lassabatere, L., Angulo-Jaramillo, R., Soria-Ugalde, J.M., Šimůnek, J., Haverkamp, R., 2009. Numerical evaluation of a set of analytical infiltration equations: EVALUATION INFILTRATION. Water Resources Research 45, n/a-n/a. https://doi.org/10.1029/2009WR007941
Lassabatere, L., Angulo-Jaramillo, R., Yilmaz, D., Winiarski, T., 2013. BEST method: Characterization of soil unsaturated hydraulic properties. In Caicedo et al. (eds): Advances in Unsaturated Soils. CRC Press, London 527–532.
Lassu, T., Seeger, M., Peters, P., Keesstra, S.D., 2015. The Wageningen Rainfall Simulator: Set-up and Calibration of an Indoor Nozzle-Type Rainfall Simulator for Soil Erosion Studies. Land Degrad. Develop. 26, 604–612. https://doi.org/10.1002/ldr.2360
Lilliefors, H.W., 1967. On the Kolmogorov-Smirnov test for normality with mean and variance unknown. Journal of the American Statistical Association 62, 399–402. https://doi.org/10.1080/01621459.1967.10482916
Liu, H., Lei, T.W., Zhao, J., Yuan, C.P., Fan, Y.T., Qu, L.Q., 2011. Effects of rainfall intensity and antecedent soil water content on soil infiltrability under rainfall conditions using the run off-on-out method. Journal of Hydrology 396, 24–32. https://doi.org/10.1016/j.jhydrol.2010.10.028
Logsdon, S.D., Jaynes, D.B., 1993. Methodology for determining hydraulic conductivity with tension infiltrometers. Soil Science Society of America Journal 57, 1426–1431.
Moldenhauer, W.C., Long, D.C., 1964. Influence of Rainfall Energy on Soil Loss and Infiltration Rates: I. Effect over a Range of Texture. Soil Science Society of America Journal 28, 813–817. https://doi.org/10.2136/sssaj1964.03615995002800060036x
Mualem, Y., Assouline, S., 1989. Modeling soil seal as a nonuniform layer. Water Resour. Res. 25, 2101–2108. https://doi.org/10.1029/WR025i010p02101
Mubarak, I., Angulo-Jaramillo, R., Mailhol, J.C., Ruelle, P., Khaledian, M., Vauclin, M., 2010. Spatial analysis of soil surface hydraulic properties:

Is infiltration method dependent? Agricultural Water Management 97, 1517–1526. https://doi.org/10.1016/j.agwat.2010.05.005
Nelson, D.W., Sommers, L.E., 1996. Total carbon, organic carbon, and organic matter, In Methods of soil analysis, part 3, chemical method, Sparks DL, et al. (eds). SSSA book series 5. Soil Science Society of America, Inc: Madison, WI; 961–1010.
Pasta, S., Badalamenti, E., Mantia, T.L., 2012. Acacia cyclops A. Cunn. ex G. Don (Leguminosae) in Italy: first cases of naturalization. Anales del Jardín Botánico de Madrid 69, 193–200. https://doi.org/10.3989/ajbm.2314
Philip, J.R., 1969. Theory of infiltration. Adv. Hydrosci., 5, 215–296.
Ramos, M., Nacci, S., Pla, I., 2000. Soil sealing and its influence on erosion rates for some soils in the Mediterranean area. Soil Science 165, 398–403.
Reynolds, W.D., 1993. Saturated hydraulic conductivity: Field measurement. M.R. Carter (Ed.), Soil Sampling and Methods of Analysis, Canadian Society of Soil Science, Lewis Publishers, Boca Raton (1993), pp. 599-613 599–613.
Reynolds, W.D., Bowman, B.T., Brunke, R.R., Drury, C.F., Tan, C.S., 2000. Comparison of tension infiltrometer, pressure infiltrometer, and soil core estimates of saturated hydraulic conductivity. Soil Science Society of America Journal 64, 478–484. https://doi.org/10.2136/sssaj2000.642478x
Reynolds, W.D., Drury, C.F., Tan, C.S., Fox, C.A., Yang, X.M., 2009. Use of indicators and pore volume-function characteristics to quantify soil physical quality. Geoderma 152, 252–263. https://doi.org/10.1016/j.geoderma.2009.06.009
Reynolds, W.D., Elrick, D.E., 1990. Ponded Infiltration From a Single Ring: I. Analysis of Steady Flow. Soil Science Society of America Journal 54, 1233. https://doi.org/10.2136/sssaj1990.03615995005400050006x
Slimene, E.B., Lassabatere, L., Šimůnek, J., Winiarski, T., Gourdon, R., 2017. The role of heterogeneous lithology in a glaciofluvial deposit on unsaturated preferential flow – a numerical study. Journal of Hydrology and Hydromechanics 65, 209–221. https://doi.org/10.1515/johh-2017-0004
Tackett, J., Pearson, R., 1965. Some characteristics of soil crusts formed by simulated rainfall. Soil Science 99, 407–413.
Touma, J., Raclot, D., Al-Ali, Y., Zante, P., Hamrouni, H., Dridi, B., 2011. In situ determination of the soil surface crust hydraulic resistance. Journal of Hydrology 403, 253–260. https://doi.org/10.1016/j.jhydrol.2011.04.004
Van Bemmelen, J., 1890. Über die Bestimmung des Wassers, des Humus, des Schwefels, der in den colloïdalen Silikaten gebundenen Kieselsäure, des Mangans usw im Ackerboden. Die Landwirthschaftlichen Versuchs-Stationen 37, 279–290.
van De Giesen, N.C., Stomph, T.J., de Ridder, N., 2000. Scale effects of Hortonian overland flow and rainfall–runoff dynamics in a West African catena landscape. Hydrol. Process. 14, 165–175. https://doi.org/10.1002/(SICI)1099-1085(200001)14:1<165::AID-HYP920>3.0.CO;2-1
van Genuchten, M.T., 1980. A closed-form equation for predicting the hydraulic conductivity of unsaturated soils. Soil science society of America journal 44, 892–898.
White, I., Sully, M.J., Melville, M.D., 1989. Use and Hydrological Robustness of Time-to-Incipient-Ponding. Soil Science Society of America Journal 53, 1343–1346. https://doi.org/10.2136/sssaj1989.03615995005300050007x
Xu, X., Kiely, G., Lewis, C., 2009. Estimation and analysis of soil hydraulic properties through infiltration experiments: comparison of BEST and DL fitting methods. Soil Use and Management 25, 354–361. https://doi.org/10.1111/j.1475-2743.2009.00218.x
Yilmaz, D., Lassabatere, L., Angulo-Jaramillo, R., Deneele, D., Legret, M., 2010. Hydrodynamic Characterization of Basic Oxygen Furnace Slag through an Adapted BEST Method. Vadose Zone Journal 9, 107. https://doi.org/10.2136/vzj2009.0039

Di Prima, S., Concialdi, P., Lassabatere, L., Angulo-Jaramillo, R., Pirastru, M., Cerda, A., Keesstra, S., 2018. Laboratory testing of Beerkan infiltration experiments for assessing the role of soil sealing on water infiltration. CATENA 167, 373–384. https://doi.org/10.1016/j.catena.2018.05.013